Chall. Nano Micro Scale Sci. Tech., 9(1): 69-80, Winter and Spring 2021
DOI: 10.22111/CNMST.2021.35450.1195

ORIGINAL RESEARCH PAPER

Forced Convective Heat Transfer of MgO/Water Nanofluid under Constant Heat Flux: Experimental and Statistical Investigation

Behrouz Raei

Department of Chemical Engineering, Mahshahr Branch, Islamic Azad University, Mahshahr, Iran

Received 20 August 2020; revised 21 March 2021; accepted 21 March 2021 available online 2 September 2021

ABSTRACT: This paper examines experimentally and statistically the heat transfer of the internal convection of MgO-water nonofluids in a copper tube for a fully turbulent regime under constant heat flux boundary condition. The Nusselt number and convective heat transfer coefficients of nonofluids in different volumetric concentrations (0, 0.05%, and 0.15%) of nonofluids were estimated. Local convective heat transfer coefficient was also observed at different points along the pipe at different Reynolds numbers. The results showed that heat transfer coefficient increased with an increase in the flow rate of nofluids from 6 to 10 l/min and the concentration of nonofluids from 0 to 0.15 vol.%. Conversely, the heat transfer coefficient decreases with increasing the nanofluid inlet temperature from 30 to 40 ˚C. At concentrations of 0.05 and 0.15% vol.% of MgO nanoparticles, the increase in the Nusselt number compared to pure water is 21.2% and 45.9%, respectively. The Taguchi method was also used to analyze the results statistically. The maximum predicted value for the Nusselt number is 114.165, and the error between the experimental value and the predicted value is 1%. Also, the concentration of nanofluid has 54.362% contribution in the Nusselt number of MgO/water nanofluid.

KEYWORDS: *Design of experiment; Heat transfer; Nanofluid; Nusselt number*

INTRODUCTION

The elimination of heat transfer produced in many products, transportation, and various constructions, has made many industrial processes challenging today. Common methods of increasing the heat sink should provide the ground for increasing the space available for heat exchange. However, they may cause the size of the heat cooling devices to increase undesirably. Among the various methods, both active and passive, nanofluids, or engineered colloidal suspension have been proven to be promising and innovative solutions thanks to their beneficial properties. Choi [1] suggested that nanoparticles should be added to the conventional heat transfer fluid (e.g., ethylene glycol, water, oil) to improve thermal properties. Since then, many scientists have turned their attention to the application of nanofluids to various geometries and heat transfer characteristics of nanofluids [2-17]. Numerous investigations have been conducted in the past on the convective heat transfer characteristics of nanofluids under constant heat flux boundary condition because they are employed in several industrial applications, some of which are addressed. Wen et al. [18] studied the forced convective heat transfer of γ-Al_2O_3 nanoparticles in a copper tube by performing a series of experiments using deionized water.

The entrance region exhibited a maximum increase in heat transfer, which decreases with an increase in the distance from the inlet. When x/D increased from 63 to 173 at Re=1600, it decreased from 47% to 14%.

Ding et al. [19] investigated heat transfer behavior of multi-walled carbon nanotubes (MWCNT) by flowing them in a horizontal tube. Their studies remarked that the concentration of CNT and the Reynolds number made good contribution to the heat transfer augmentation. Their results clearly indicate that CNTs having 0.5 wt% and at Reynolds number of 800, a maximum enhancement of 350% is achieved. Chen et al. [20] conducted a series of experimental studies to predict heat transfer coefficients and investigate the behavior of titanium nanotubes. They also performed some experiments to explore various factors, including effective thermal conductivity, forced convective heat transfer, and rheological behavior of nanofluids. Only a maximum of 5% enhancement was observed by the titanate nanofluids under particle loading of 2.5 wt%. Kayhani et al. [21] examined the pressure drop and heat transfer in a turbulent flow of the aqueous solution of TiO_2 nanoparticels, which flowed in a constantly heated horizontal circular tube containing 0.1, 0.5, 1.0, 1.5 and 2.0% volume concentrations of nanoparticles. The results showed an increase in heat transfer coefficient as a result of increased nanofluid volume fraction. The Nusselt number was also found increased to be about 8% for nanofluid at a Reynolds number of 11800, with 2.0% nanoparticles volume fraction. Heat transfer coefficient and friction factor with SiO_2/water nanofluid up to 4% particle volume concentration were determined by Azmi et al. [22].

*Corresponding Author Email: *b.raei@mhriau.ac.ir*

Note. This manuscript was submitted on August 20, 2020; approved on March 21; published online September 2, 2021.

Nomenclature

C	concentration (vol.%)
Cp	specific heat at constant pressure (J/kg.K)
D	diameter (mm)
h	heat transfer coefficient (W/m^2.K)
h_x	local heat transfer coefficient (W/m^2.K)
K	thermal conductivity
l	liter
L	level
m	number of experiments
$MAPE$	mean absolute percentage error
n	number of repetitions
Nu	Nusselt number
P	percent of contribution
Pr	Prandtl number
PC	personal computer
PID	proportional–integral–derivative
PVC	polyvinyl chloride
Q	nanofluid flow rate, (l/min)
Re	Reynolds number
T	temperature, (°C)
V	variance
Y	value of results
$\bar{Y}$	average value of results

Greek Letters

μ	viscosity (mPa.s)
ρ	density (kg/m^3)

Subscripts

bf	base fluid
Er	error
F	factor
nf	nanofluid
P	particle

At a volumetric concentration of 3%, they saw an increasing and then a decreasing trend in heat transfer coefficients.

At this volumetric concentration, the maximum increase in the Nusselt number was approximately 38% within the Reynolds range. Esfe and Saedodin [23] conducted a series of experimental studies on dynamic viscosity, Nusselt number, and thermal conductivity of turbulent forced convection of MgO-water nanofluids flowing in a circular tube. The pure water and nanofluid with the nanoparticle volume fraction of 0.005, 0.01, 0.015, and 0.02 and the nanoparticles diameter of 20,40,50 and 60 nm were considered. Experimental results showed a tendency of heat transfer to increase due to the presence of nanoparticles in pure water. Ali [24] experimentally tested the internal convective heat transfer of SiO_2-water nanofluids flowing in a copper tube for a fully turbulent regime. He also determined the local convective heat transfer coefficient in different positions along the pipe in different Reynolds numbers. The maximum increase was 8-9% at 0.001 vol% SiO_2 nanoparticles. However, convective heat transfer coefficient increased by 27% at 0.007 vol% SiO_2 nanoparticles. Abdolbaqi et al [25] studied the forced convection heat transfer of CuO, TiO_2 and Al_2O_3 under turbulent flow through a straight square. The boundary conditions were applied under a 5000 W/m^2 heat flux, the Reynolds number 10^4-10^6, and a constant volume concentration of 1 to 4%.

The results suggested an increase in heat transfer and wall shear stress with increasing nanofluid volume concentration. CuO nanofluids appear to increase heat transfer significantly. The study remarked the enhancement of the friction factor and the Nusselt number is 2% and 21%, respectively, for the channel at all Reynolds numbers. Hemmat Esfe [26] et al. reported results of experiments on thermal conductivity, viscosity and turbulent heat transfer behavior of MgO–water nanofluid in a straight circular tube for the volume fraction of nanoparticles <1%. They observed that most of the conventional models fail to predict the thermal conductivity and dynamic viscosity of the MgO–water nanofluid accurately.

Their results indicated that addition of low value of nanoparticles to the base fluid results in enhanced heat transfer. As observed in the literature review, the heat transfer properties of MgO nanoparticles have been less studied than those of other metal oxide nanoparticles (e.g., Al_2O_3, TiO_2, and CuO). On the other hand, lack statistical analysis exists on the operating parameter. The majority of researchers indicated that nanoparticle concentration, temperature, and nanofluid flow rate (Reynolds number) affect heat transfer coefficient. Nevertheless, nothing could be understood by comparing the operational parameters. The present study includes an experimental study of the convective heat transfer of MgO-water nanofluids, which passes through a copper tube in a fully turbulent regime under constant heat flux conditions. Nusselt number and convective heat transfer coefficient were investigated in a very dilute concentration of nanoparticles. Local convective heat transfer coefficient was also observed at various points along the pipe. The main objectives of this study are three-fold: 1) to assess the impact of each parameter on the Nusselt number and local heat transfer coefficient and 2) to apply the statistical Taguchi experimental design method on the optimization of factors and to find a combination of parameters to achieve the maximum value of the Nusselt number and 3) to examine all the interaction effects of factors.

PREPARATION OF THE NANOFLUID

MgO nanoparticles with distilled water (as a base fluid) are used in this work. Nanoparticles are manufactured by the US Nanomaterials Research Company, USA. The specifications of the nanoparticles are shown in Table 1.

Here, a transmission electron microscope (TEM) has been used to approximate the shape and size of MgO nanoparticles.

Figure 1 demonstrates that the shape and size of nanoparticles are approximately spherical and around 20nm, respectively. Many researchers employ this method [27-28].

Table1
Specification of nanoparticle used in this study

Nanoparticle	Magnesium Oxide (MgO)
Average particle size (nm)	20
Purity	>98%
Density (kg/m^3)	3580
Color	white
Morphology	nearly spherical
Specific area(m^2/g)	>60
Specific heat (J/kgK)	880
Thermal conductivity (W/mK)	45

There are two methods, i.e., single-step and two-step, for nanofluid production. Providing stable nanofluid is a challenge. Various methods are used to achieve stable nanofluid, including changes in nanofluid pH, the addition of surfactants, and ultrasonic vibration. In this study, nanofluid was prepared with a concentration of 0.05 and 0.15 of vol%. A specific amount of MgO nanoparticles is weighed (accurate to three decimal places) to which distilled water was added as a base fluid. After one hour of mixing with a magnetic stirrer, the nanofluid was put in a ultrasonic vibrator (BANDELIN Company with a power = 240 kW and frequency = 35 kHz) for 5 hours. This procedure is utilized to create a stable suspension system of nanofluid and break the agglomeration of nanoparticles in fluid. The prepared solution remains stable at static condition for 3 day after experimentation. No surfactant was utilized in the study as it may have affected the thermal conductivity of nanofluids [29-30]. Repeatability was assessed during the experiments. Some experiments were randomly repeated at various points in times, revealing a slight difference between the two. That is, over time, there has been no change in test results, indicating nanofluid stability.

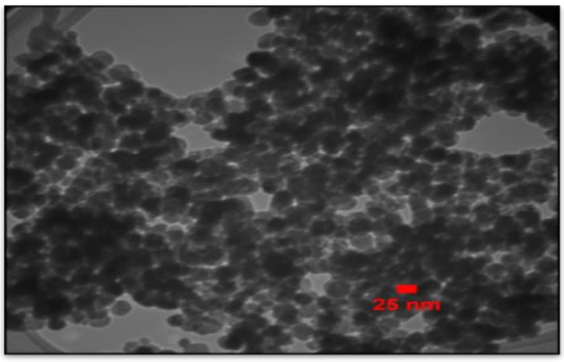

Fig. 1. TEM image of MgO nanoparticles

EXPERIMENTAL SETUP

The schematic and realistic view of the experimental apparatus is illustrated in Figure 2 a, b. This test loop is designed to study the internal convective heat transfer in the fully developed turbulent flow domain.

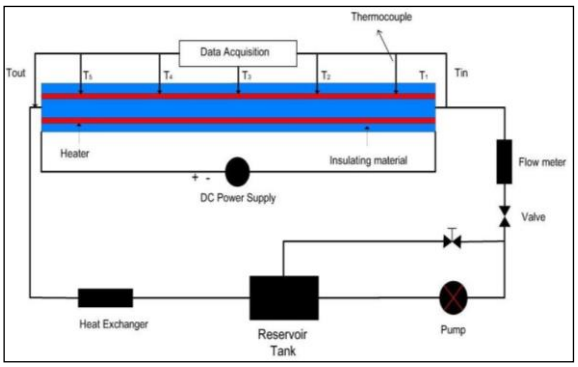

(a)

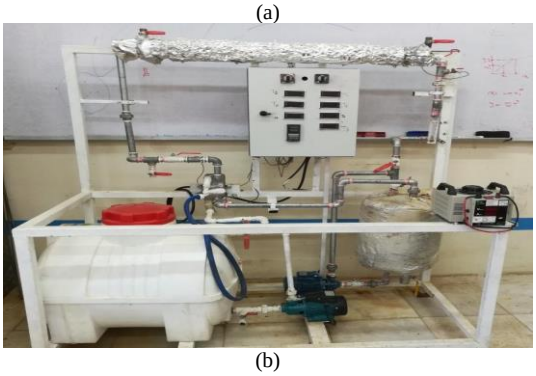

(b)

Fig.2. a) Schematics of the experimental setup **b)** photograph of the experimental setup

DATA REDUCTION

Prior to the experiments, MgO nanoparticles were dispersed in distilled water with 0.05 and 0.15 vol.% in order to produce nanofluids. The thermophysical properties of nanofluids were investigated at mean bulk temperatures. The values of density, heat capacity, thermal conductivity, and viscosity for nanofluids were calculated by equations (1-4) [32-35].

$$\rho_{nf} = \emptyset\rho_p + (1-\emptyset)\rho_{bf} \quad (1)$$

$$CP_{nf} = \frac{(1-\emptyset)P_{bf}CP_{bf} + \emptyset P_p CP_p}{P_{nf}} \quad (2)$$

$$K_{nf} = \frac{K_p + 2K_{bf} - 2\emptyset(K_{bf} - K_p)}{K_p + 2K_{bf} + \emptyset(K_{bf} - K_p)} K_{bf} \quad (3)$$

$$\mu_{nf} = (1 + 2.5\emptyset)\mu_{bf} \quad (4)$$

The thermophysical properties are used to appraise the convective heat transfer coefficient and Nusselt number of base fluid and nanofluids at different volume concentrations. Given the excellent insulation of the test section and disregard of heat loss, heat flow can be equated with the power input. The supplied heat for the test section can be calculated as follows:

$$Q_a = V \times I \tag{5}$$

Heat absorbed by the nanofluid can be appraised as:

$$Q_b = \dot{m} C_p (T_{out} - T_{in}) \tag{6}$$

where "T_{out}" and "T_{in}" are the temperatures at the outlet and entry of the test section, respectively. Heat flux is given by:

$$q'' = \frac{Q}{\pi D L} \tag{7}$$

In the above equation, D, L, and Q are the inner diameter of the copper tube, the test section length, and the rate of heat transfer, respectively, which can be measured using equation 8:

$$Q = \frac{Q_a + Q_b}{2} \tag{8}$$

The average convective heat transfer coefficient "h" of the working fluids can be calculated by:

$$h = \frac{q''}{T_s - T_m} \tag{9}$$

where,

$$T_m = \frac{T_{in} + T_{out}}{2} \tag{10}$$

And

$$T_s = \frac{(\sum_{n=1}^{5} T_n)}{5} \tag{11}$$

where T_m and T_s are the average bulk and surface temperatures, respectively. Nusselt number can be measured as follows:

$$Nu = \frac{h \times D}{K_{nf}} \tag{12}$$

Now in order to calculate the local heat transfer coefficient and local Nusselt number, replace "h" by h(x) and Nu by Nu(x). The values can be calculated as:

$$h(x) = \frac{q''}{T_s(x) - T_m(x)} \tag{13}$$

$$Nu(x) = \frac{h(x) \times D}{K_{nf}} \tag{14}$$

In the above equation, $T_m(x)$ can be given as:

$$T_m(x) = T_{m,i} + \frac{q'' P}{(\dot{m} \times C_p)} x \tag{15}$$

P, m, and x are the perimeter, mass-flow rate, and the axial distance from the test section entrance, respectively.

UNCERTAINTY ANALYSIS

Uncertainty analysis was performed to estimate the error in the calculations due to fluctuations in the measurements. Moffat [36] method was used to assess the uncertainty of the experimental data. The uncertainties in the experimental results can be designated by calculating the deviation of the parameters, such as flow rate, mass, wall temperature, bulk temperature, voltage, current, diameter, and length. Thereafter, the error of each parameter was incorporated into the estimation of uncertainties. The uncertainties in the values estimated are summarized and presented in Tables 2 and 3.

Table 2
Uncertainties of instruments.

Variable	Uncertainty/%
Voltage/V	1
Current/I	0.25
Thermocouple/°C (wall temperature)	0.32
Thermocouple/°C (fluid temperature)	0.46
Volume/ml	0.1
Length of tube/m	0.33
Diameter/m	1.25
Time/s	0.01

Table 3
Uncertainties of parameters and variables.

Parameter	Uncertainty/%
Mass flow rate	0.8
Reynolds number	1.1
Heat transfer coefficient	7.2
Nusselt number	7.8
Heat flux	1.8
Concentration	0.1

DESIGN OF EXPERIMENTS

The Taguchi method involves reducing the variation in a process through robust design of experiments. The overall goal is to create a high-quality, low-cost product [37]. This

method is an essential tool for designing and analyzing systems. It is mainly based on using standard tables known as orthogonal arrays (OA) for experimental design. The main characteristic of the above method is that it examines various parameters that affect the system performance using a small number of experiments. QUALITEK-4 (QT4) software was used to analyze the results and optimize the conditions to determine the control factors. QUALITEK-4 (QT4) version 4.75 is the windows version software for automatic design and analysis of Taguchi experiments. In this work, three controllable factors are considered, including the nanofluid flow rate, nanofluid concentration, and nanofluid temperature, each with three levels (Table 4).

Table 4
Parameters and levels.

Parameters	Labels	Level1	Level2	Level4
Nanofluid concentration/vol%	C	0	0.05	0.15
Nanofluid temperature/ °C	T	30	35	40
Nanofluid flow rate/ l/min	Q	6	8	10

If a full factorial experimental design is employed, the permutations number would be 3^3. Nevertheless; the number of tests was reduced to 9 by the fractional factorial design. An L_9 OA represented in Table 5 is selected, where subscript 9 and L denote the number of experiments and the Latin square, respectively. Each row of the matrix specifies a run. In Table 5, the numbers 1, 2, and 3 represented the 1st, 2nd, and 3rd levels of a factor, respectively. Therefore, the experimental results (Nusselt number) in Table 5 are achieved by combining the values of the levels in Table 4 and L9 OA.

Table 5
L_9 array selected for experiments and the corresponding experimental results.

Factors levels Run no	C	T	Q	Nu
1	1	1	1	75.2
2	1	2	2	70.4
3	1	3	3	74.9
4	2	1	2	83.7
5	2	2	3	88.5
6	2	3	1	69.3
7	3	1	3	115.5
8	3	2	1	87.2
9	3	3	2	88.9

Consequently, a standard analysis is applied to utilize the average results to assess the empirical results. Generally, for standard analysis, selecting a quality characteristic (QC) is required only to determine the optimal condition. Tree kinds of QC are appropriate in this regard: 1) lower-the-better (LB), 2) nominal-the-best (NB), and 3) higher-the-better (HB). Since this study aims to attain the highest value of the Nusselt number of MgO-water nanofluid, the QC with HB is needed.

RESULTS & DISCUSSIONS

Validation of the Experimental Setup

To verify the accuracy of the experimental setup, distilled water was utilized as a working fluid, and the forced convective heat transfer coefficient in the turbulent flow regime was measured. The experimental results were compared with the prediction of Gnielinski [38] and Dittus-Boelter [39] correlations shown as equations 16 and 17,respectively :

$$Nu_D = \frac{\left(\frac{f}{8}\right)(Re_D - 1000)Pr}{1 + 12.7\left(\frac{f}{8}\right)^{\frac{1}{2}}\left(Pr^{\frac{2}{3}} - 1\right)} \quad (16a)$$

$$f = (0.79 ln Re_D - 1.64)^{-2} \quad (16b)$$

which is considered valid within the range $0.5<Pr<2000$ and of $2300<Re<5\times10^6$.

$$Nu = 0.0236 Re^{0.8} Pr^{0.3} \quad (17)$$

Figure 3 illustrates a comparison between experimental test data and Gnielinski and Dittus-Boelter correlations. Mean absolute percentage error (MAPE) of the prediction of Gnielinski and Dittus-Boelter correlations are 17% and 14%, respectively. There is an reasonable agreement between the calculated values and the experimental results for distilled water.

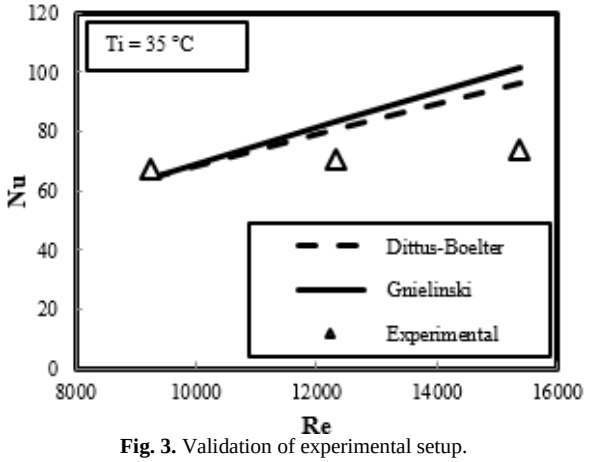

Fig. 3. Validation of experimental setup.

Convective heat transfer

In the present study, the turbulent forced convective heat transfer of MgO/distilled water nanofluids passing through a

circular tube considering uniform heat flux boundary condition is experimentally measured. In the present investigation, MgO/distilled water nanofluids with three volume concentrations (0, 0.05, 0.15 vol%) were used. Figure 4 shows the average heat transfer coefficient for nanofluid and water at different volume fraction, temperature, and Reynolds number. The results showed that nanofluids have an average heat transfer coefficient higher than the base fluid, and the average heat transfer coefficient increases with volume fraction of nanoparticles and decreases with increasing temperature of nanofluids. Also, the average heat transfer coefficient of nanofluids and water increases with increasing Reynolds number.

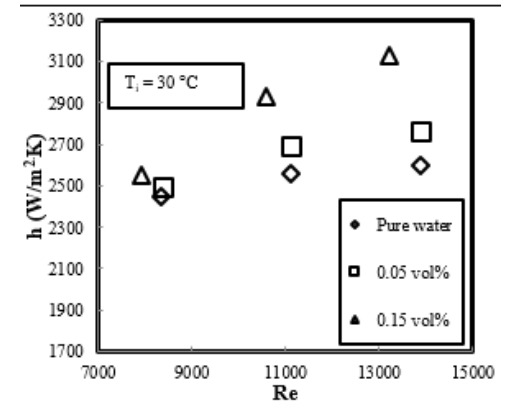

(a)

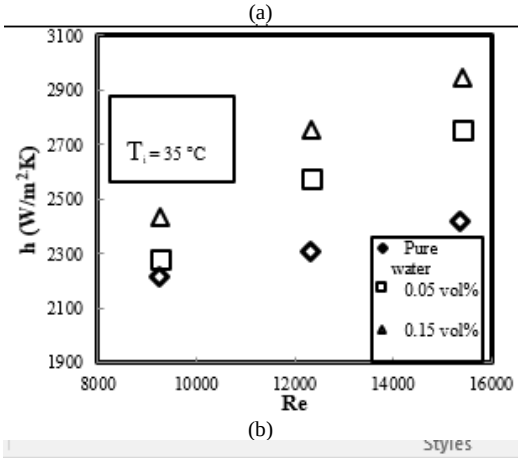

(b)

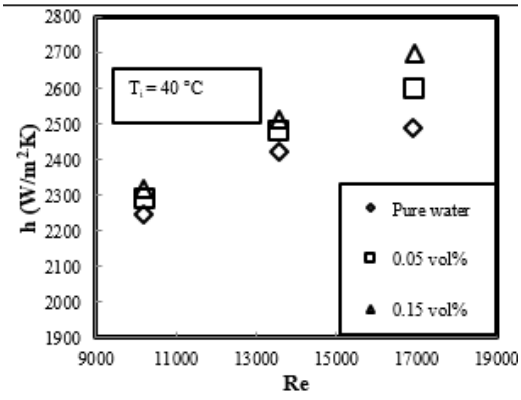

(c)

Fig. 4. Variation of average heat transfer coefficient of nanofluid with Reynolds number at the inlet temperatures of a) 30 °C, b) 35 °C, and c) 40 °C

In addition, increase in the volume concentration of nanoparticles causes higher thermal conductivity that motivates increase of heat transfer coefficient of nanofluid.

Therefore, adding nanoparticles to the base fluid may result more number of collisions due to the Brownian motion of particles. Also, particle migration and reduction of boundary thickness may be the reason of increase in nanofluid heat transfer. Although Previous researchers have suggested that the heat transfer of nanofluids increases due to many factors, including mixed effects of Brownian particle motion, near-wall particles, particle migration, reduced boundary-layer thickness, and thermal conductivity enhancement [40-41]. According to Figure 4, by increasing the fluid inlet temperature, the average heat transfer coefficient of nanofluid can be reduced. This decrease in the average heat transfer coefficient of the nanofluid with increase in nanofluid inlet temperature can be due to two factors: first, rapid alignment of nanoparticles in lower viscosity fluids, leading to less contact between nanoparticles. Second, depletion of particles in the near-wall fluid phase [42], leading to an intrinsically lower thermal conductivity layer at the wall. Knowing which mechanism or mechanism may be responsible for the experimental results requires important future work, including computational fluid dynamic modeling of the flows in nanoparticle dispersions.

Table 6 shows enhancement of Nusselt number of nanofluid compared to the base fluid (in percent) at different volume fraction, temperature, and Reynolds number. In case of 0.15% MgO nanoparticles, temperature and Reynolds number equal 30 °C and 13872, respectively, maximum value of enhancement of Nusselt number was observed. An increased Reynolds number also increases the Nusselt number. The observed value of Reynolds number was approximately 8300–17000, and the regime was fully turbulent. An approximately 45.9% increase in the Nusselt number, compared with the base fluid in the Reynolds number 13872 for 0.15% MgO nanoparticles, was observed. In the case of 0.05% of MgO nanoparticles, the maximum observed increase was 21.2%.

Table 6
Enhancement of Nusselt number of nanofluid compared to the base fluid (in percent).

T_i (°C)	Re	φ = 0.05%	φ = 0.15%
30			
	8341	9.1	28.7
	11109	15.3	34.5
	13872	21.2	45.9
35			
	9252	6.4	21.4
	12311	11.8	28.5
	15373	14.1	40.4
40			

	10172	2.9	15.7
	13551	8.1	22
	16924	10.3	30.9

Local convective heat transfer coefficient

Figure 5 depicts the local convective heat transfer coefficient versus the axial distance of the test section at three different volumetric flow rates. It can be seen that the maximum increase can be seen at the test section entrance, and it decreases as approaches to the end of the test section. It occurs due to changes in the thermal boundary layer thickness at this distance.

The thickness of the thermal boundary layer and the resulting thermal resistance is low at the inlet of the test section.

It causes heat transfer coefficient to increase. Conversely, at the end of the test section, the thermal boundary layer and thermal resistance increase, this results in a reduction of the heat transfer coefficient. Also, compared with pure water, when the nanoparticles concentration increases, heat transfer coefficient rises. It can be observed that increasing the fluid flow rate from 6 to 10 l/min causes heat transfer coefficient to increase. Increasing fluid flow rate increases Reynolds number and consequently increases the turbulence and better dispersion of nanoparticles in the liquid bulk. As a result, the temperature distribution is flattened, and the temperature gradient between the heat transfer surface and the working fluid is sharpened.

In Figure 6, bulk and wall axial temperature profiles along the test pipe are shown at the 4.5 kW/m^2 power supply for the MgO-water nanofluid at 0.15% volume concentration and three inlet temperatures include 30,35 and 40 °C. The temperature difference between wall and bulk raises with axial distance.

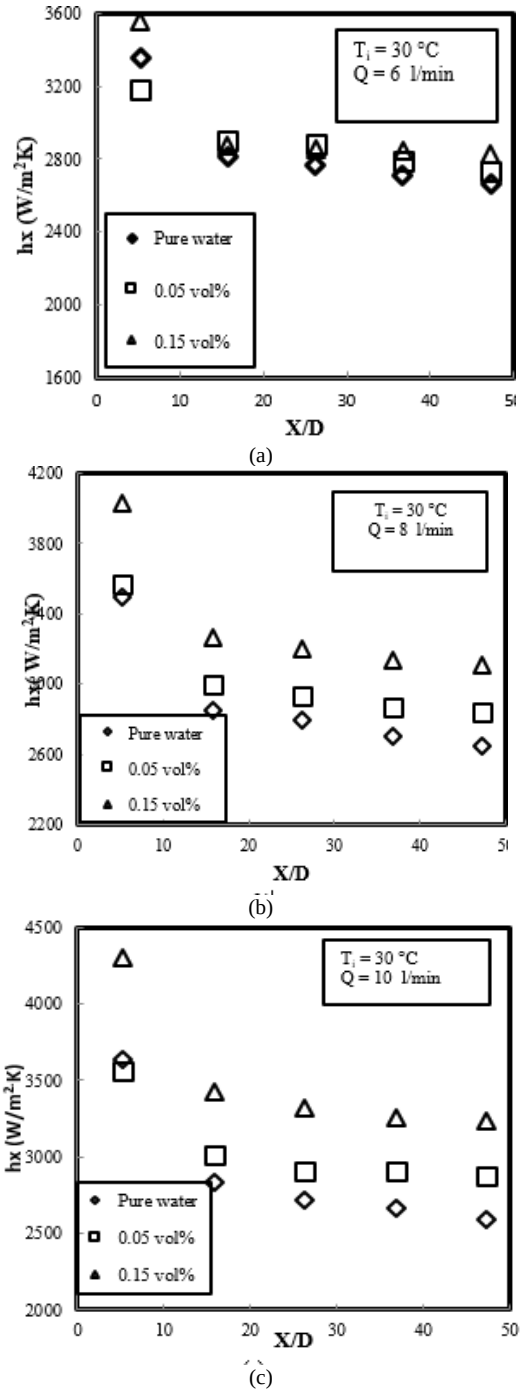

Fig. 5. Local heat transfer coefficient variation of MgO/water nanofluid along axial distance at Ti = 30 °C, a) Q= 6 l/min, b) Q = 8 l/min, c) Q = 10 l/min

STATISTICAL ANALYSIS

Main Effects

Using Qualitek-4 (QT4) software, the results were analyzed and the conditions were optimized for setting the control factors. Based on the Taguchi method in Table 5, implementations 1-9 were run. The main impact of control factors in the Taguchi method represents the trend of the effect of a factor. The average results were used to calculate the main effects. The impacts of the nanofluid flow rate, temperature, and concentration on the Nusselt number are shown in Figure 7 (a,b and c).

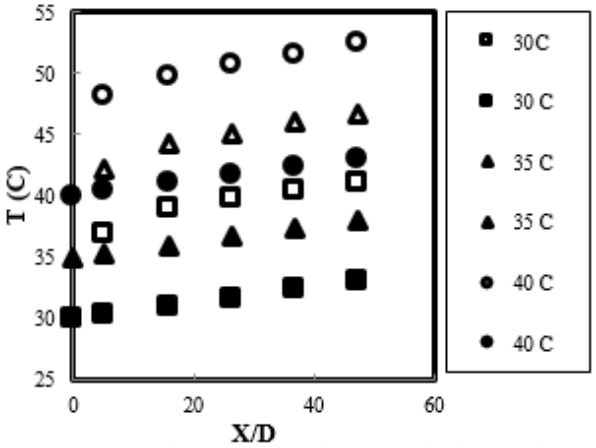

Fig. 6. Bulk and wall temperature profiles versus the dimensionless axial length, for three inlet temperatures include 30,35 and 40 °C, MgO-water nanofluid at 0.15 vol.% concentration and flow rate of 6 l/min and Nominal heat flux 4.5 kW/m^2.(■,●,▲) Bulk and (□,○,Δ) wall temperatures.

Figure 7a represents the effect of the nanofluid flow rate on the average response value. As observed, by increasing the nanofluid level from level 1 to level 3 (from 6 to 10 l/min), the average response value increases, which is the Nusselt number at each level. The highest value occurs at level 3 (10 l/min), where the average response is 93. Hence, to achieve the optimal response value, the nanofluid flow rate must be increased. Figure 7b indicates that increasing the nanofluid temperature level from 1 to 3 (from 30 ˚C to 40 ˚C) has a negative effect on the average response value at each level. Indeed, to obtain the maximum response value, the nanofluid temperature must be set to the first level (30˚C).Figure 7c shows the effect of nanofluid concentration on the average response value. As predicted, by increasing the concentration level from 1 to 3 (from 0 to 0.15 vol.%), the average response increased at each level and reached the highest value (97.2) at level 3.

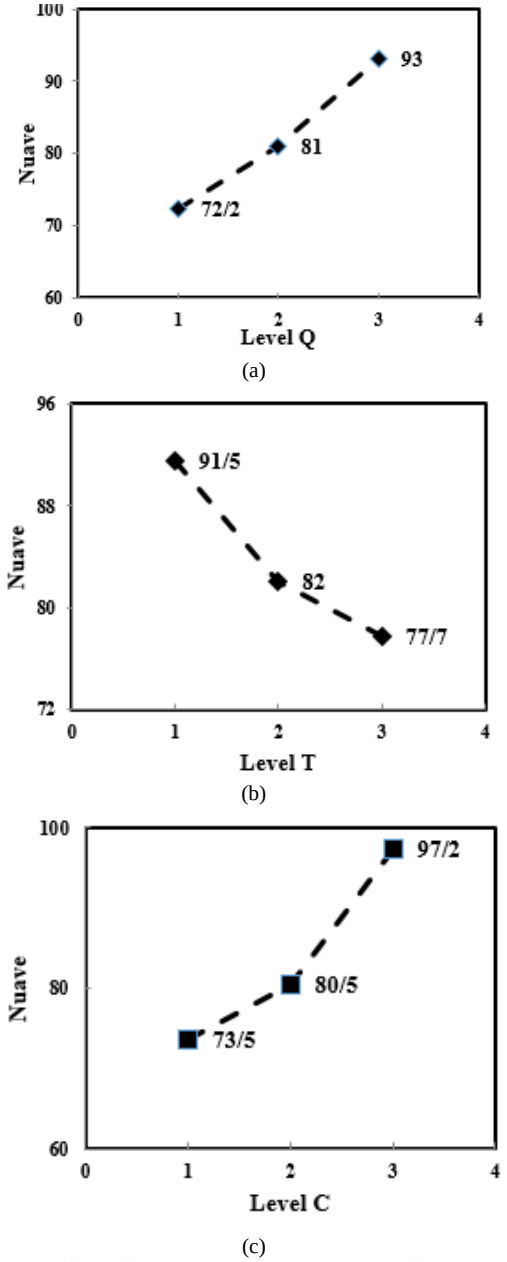

Fig. 7. Effect of factors on the Nusselt number a) flow rate b) Temperature c) Concentration

RESULTS OF ANALYSIS OF VARIANCE (ANOVA)

ANOVA is another technique used to optimize the results proposed by the Taguchi method. These data represent the interactions and the relative effects of the factors on the variation of the results. Information obtained from ANOVA will indicate the contribution of individual factors and interactions on the result and performance of system.

P_F denotes the percentage contribution of each factor as follows:

$$P_f = \frac{SS_f - (DOF_F V_{Er})}{SS_T} \times 100 \quad (18)$$

where DOF_F denotes the degree of freedom for each factor obtained by subtracting one from the number of each factor's level (L). The total sum of squares (SS_T) is calculated as follows:

$$SS_T = \sum_{j=1}^{m} \left(\sum_{i=1}^{n} Y_i^2 \right)_j - mn(\bar{Y}_T)^2 \quad (19)$$

where

$$\bar{Y}_T = \sum_{j=1}^{m} \frac{(\sum_{i=1}^{n} Y_i)_j}{mn} \quad (20)$$

where m, n, and Y_i show the number of tests carried out, the number of repetitions in identical experimental conditions, and the value of the measurement results of a definite run, respectively.

The factorial sum of squares (SS_F) [43] can be measured as follows:

$$SS_F = \frac{mn}{l} \sum_{k=1}^{L} (\bar{Y}_k^F - \bar{Y}_T)^2 \quad (21)$$

where $\bar{Y}_k^F$ is the average value of the measurement results of a certain factor in the "kth" level. The variance associated with each factor (V_F) can be calculated as follows:

$$V_F = \frac{SS_F}{DOF_F} \quad (22)$$

Also, the variance of error, V_{Er}, is:

$$V_{Er} = \frac{SS_T - \sum_{F=A}^{D} SS_F}{m(n-1)} \quad (23)$$

Initially, $\bar{Y}_k^F$ was attained from the response column in Table 5. By replacing $\bar{Y}_k^F$ and $\bar{Y}_T$ into equation 21, the factorial sum of squares, SS_F, for each factor was individually determined. Utilizing equation 19, the total sum of squares, SS_T, was calculated. Replacing DOF_F and SS_F in equation 22, the variance of each factor was obtained, and the variance of error, V_{Er}, was attained by replacing SS_T and SS_F into equation 23. Ultimately, by replacing DOF_F=2, SS_T, and SS_F into equation 18, the percentage contribution of each factor, P_F, was defined. These values are demonstrated in Table 7. The most explanatory part of the ANOVA table is the percent of contribution that each factor or interaction makes with the view to optimize the system and consequent results. Also, the other/error row includes the data regarding the sources of results variability. This row represents the information regarding the effects from three sources: 1) uncontrollable factors (noise), 2) the factors not involved in the test, and 3) experimental error. The contribution of each factor on Nusselt number P_F is provided in Table 7. It is observed that the nanofluid concentration is the most effective factor in the response (Nusselt number) with 54.362%, followed by flow rate and temperature of nanofluid with 24.212% and 17.517%, respectively.

The optimal conditions for the test can be obtained by applying the ANOVA. The performance at optimal conditions is determined in terms of the selected QCs using the QT4 software. Table 8 represents the best performance and optimal conditions for our case study. Based on the Taguchi method, the nanofluid concentration possesses the most significant determinant of the Nusselt number with 13.466. The best set for control factors is as follows: nanofluid concentration, temperature, and flow rate set to 0.15 vol.%, 30℃, and 10 l/min, respectively. The current grand average (i.e., arithmetic mean for all trials) for the Nusselt number is around 83.733.Nevertheless, at optimal conditions, the Nusselt number is increased to about 114.165.

Table 7
ANOVA for the Nusselt number.

Factor	DOF_F	SS_T	V_F	SS_F	P_F,%
C	2	889.582	444.791	873.880	54.362
T	2	297.289	148.664	281.586	17.517
Q	2	404.925	202.462	389.223	24.212
other/error	2	15.701	7.850		3.909
Total	8	1607.499	-		100

Table 8
Optimum conditions and performance of the Nusselt number.

Factor	Level Description	Level	Contribution
C	0.15	3	13.466
T	30	1	7.773
Q	10	3	9.233
Total contribution of all factors			30.431
Current Grant Average of Performance			83.733
Expected Result at Optimum Condition			114.165

Confirmation Test

Upon determining optimal conditions through statistical analyses, a confirmation test was performed under such circumstances to evaluate the accuracy of the predicted results. Table 9 provided the results. It is observed that there is a good consistency between the results of the current experiment and those of the statistical model.This demonstrates a good consistency between the experimental and the predicted values, with only a 1% error, and approves the effectiveness of the experimental design to attain the optimal value of the Nusselt number in only 9 runs instead of 27. However, this study uses the Taguchi method for statistical analysis of the experimental results and reduce the number of experiments is not the main aim.

Table 9
Results of confirming the experiment and statistical model at optimum conditions.

Operating conditions			Predicted result	Experimental result,
Concentration, Vol.%	Temperature, °C	Flow rate, l/min		
0.15	30	10	114.165	115.5

Interaction

Factors A and B interact when changes in level A alter the effect of B and vice versa. For "n" control factors in a DOE, the total number of interaction is n(n-1)/2.Here, three control factors yield three interactions. The criterion for the significance of an interaction is called severity index (SI) which helps to understand the influence of two individual factors at various levels of interaction.The results are provided in Table 10. In mentioned Table "column" represents the location of the main factors comprising the interaction. The "reserved" column refers to the column to which the studied interactions are assigned. "Levels" shows the factor levels desirable to obtain the optimum result. According to the Table 10, temperature and flow rate possess the highest SI (27.38%).

Table 10
Severity index for two factors.

No	Factors label	Columns	SI (%)	Reserved	Levels
1	T×Q	2×3	27.38	1	[1,3]
2	C×Q	1×3	20.77	2	[3,3]
3	C×T	1×2	10.38	3	[3,1]

CONCLUSIONS

This research article presents an experimental investigation on the convective heat transfer characteristics of MgO/water nanofluids in turbulent flow through a horizontal copper tube under constant heat flux at different nanofluid volumetric flow rates, various nanofluid concentrations and several inlet temperatures of the nanofluid. Also, the results have been statistically analyzed using Taguchi method. The major conclusions are as follows:

- The heat transfer coefficient increases with enhancing volumetric flow rate of the nanofluid significantly but decreases with increasing inlet temperature of the nanofluid.
- By adding nanoparticles to the base fluid, the Nusselt number increases. At concentrations of 0.05 and 0.15% vol.% of MgO nanoparticles, the increase in the Nusselt number compared to pure water is 21.2% and 45.9%, respectively.
- According to the analysis performed using Taguchi method, the best operating conditions includes minimum temperature, maximum concentration of nanofluid and maximum flow rate of nanofluid.
- The maximum predicted value for the Nusselt number is 114.165, and the error between the experimental value and the predicted value is 1%.
- The concentration of nanofluid has 54.362% contribution in the Nusselt number of MgO/water nanofluid. Nanofluid volumetric flow rate and temperature of nanofluid have 24.212% and 17.517% contribution in the Nusselt number of MgO /water nanofluid, respectively.

Agglomeration, high cost, instability, and size of nanoparticles are some of the significant problems faced by researchers working with nanofluids. This limits the use of nanofluids in specific applications, such as industrial heat exchangers. Therefore, a new technique for the long-term stability of nanoparticles dispersion must be established. Also, new mass-production techniques and methods need to be considered to produce nanofluids at an affordable cost so that they can be utilized in the markets.

REFERENCES

[1] Choi SUS. editor Enhancing thermal conductivity of fluids with nanoparticles. Proceedings of the 1995 ASME International Mechanical Engineering Congress and Exposition; 1995; New York, USA.

[2] Raei B, Shahraki F, Jamialahmadi M, Peyghambarzadeh S. Experimental study on the heat transfer and flow properties of γ-Al2O3/water nanofluid in a double-tube heat exchanger. J Therm Anal Calorim. 2017;127(3):2561-75.

[3] Raei B, Peyghambarzadeh SM. Measurement of Local Convective Heat Transfer Coefficient of Alumina-Water Nanofluids in a Double Tube Heat Exchanger. Journal of Chemical and Petroleum engineering. 2019;53(1):25-36.

[4] Vermahmoudi Y, Peyghambarzadeh SM, Hashemabadi SH, Naraki M. Experimental investigation on heat transfer performance of /water nanofluid in an air-finned heat exchanger. European Journal of Mechanics - B/Fluids. 2014;44(0):32-41.

[5] Peyghambarzadeh SM, Hashemabadi SH, Naraki M, Vermahmoudi Y. Experimental study of overall heat transfer coefficient in the application of dilute nanofluids in the car radiator. Appl Therm Eng. 2013;52(1):8-16.

[6] Darzi AAR, Farhadi M, Sedighi K. Heat transfer and flow characteristics of AL_2O_3–water nanofluid in a double tube heat exchanger. Int Commun Heat Mass. 2013;47(0):105-12.

[7] Zamzamian A, Oskoui SN, Doosthoseini, Joneidi A, Pazouki M. Experimental investigation of forced convective heat transfer coefficient in nanofluids of Al2O3/EG and CuO/EG in a double pipe and plate heat exchangers under turbulent flow. Exp Therm Fluid Sci. 2011;35(3):495-502.

[8] Anoop K, Sadr R, Yu J, Kang S, Jeon S, Banerjee D. Experimental study of forced convective heat transfer of nanofluids in a microchannel. Int Commun Heat Mass. 2012;39(9):1325-30.

[9] Malvandi A, Ghasemi A, Ganji D. Thermal performance analysis of hydromagnetic Al_2O_3-water nanofluid flows inside a concentric microannulus considering nanoparticle migration and asymmetric heating. Int J Therm Sci. 2016;109:10-22.

[10] Malvandi M, Ganji DD. Brownian motion and thermophoresis effects on slip flow of alumina/water nanofluid inside a circular microchannel in the presence of a magnetic field. Int J Therm Sci. 2014;84:196-206.

[11] Tiwari AK, Ghosh P, Sarkar J. Heat transfer and pressure drop characteristics of CeO_2/water nanofluid in plate heat exchanger. Appl Therm Eng. 2013;57(1–2):24-32.

[12] Pandey SD, Nema VK. Experimental analysis of heat transfer and friction factor of nanofluid as a coolant in a corrugated plate heat exchanger. Exp Therm Fluid Sci. 2012;38(0):248-56.

[13] Lotfi R, Rashidi AM, Amrollahi A. Experimental study on the heat transfer enhancement of MWNT-water nanofluid in a shell and tube heat exchanger. Int Commun Heat Mass. 2012;39(1):108-11.

[14] Ghozatloo A, Rashidi A, Shariaty-Niassar M. Convective heat transfer enhancement of graphene nanofluids in shell and tube heat exchanger. Exp Therm Fluid Sci. 2014;53(0):136-41.

[15] Anoop K, Cox J, Sadr R. Thermal evaluation of nanofluids in heat exchangers. Int Commun Heat Mass. 2013;49(0):5-9.

[16] Zangeneh A, Vatani A, Fakhroeian Z, Peyghambarzadeh S. Experimental study of forced convection and subcooled flow boiling heat transfer in a vertical annulus using different novel functionalized ZnO nanoparticles. Appl Therm Eng. 2016.

[17] Raei B, Shahraki F, Jamialahmadi M, Peyghambarzadeh SM. Experimental investigation on the heat transfer performance and pressure drop characteristics of γ-Al2O3/water nanofluid in a double tube counter flow heat exchanger. Transport Phenomena in Nano and Micro Scales. 2016;5(1):64-75.

[18] Wen D, Ding Y. Experimental investigation into convective heat transfer of nanofluids at the entrance region under laminar flow conditions. Int J Heat Mass Transfer. 2004;47(24):5181-8.

[19] Ding Y, Alias H, Wen D, Williams RA. Heat transfer of aqueous suspensions of carbon nanotubes (CNT nanofluids). Int J Heat Mass Transfer. 2006;49(1):240-50.

[20] Chen H, Yang W, He Y, Ding Y, Zhang L, Tan C, et al. Heat transfer and flow behaviour of aqueous suspensions of titanate nanotubes (nanofluids). Powder Technol. 2008;183(1):63-72.

[21] Kayhani MH, Soltanzadeh H,M. M. Heyhat., M. Nazari. and F. Kowsary., Experimental study of convective heat transfer and pressure drop of TiO_2/water nanofluid. Int Commun Heat Mass. 2012;39(3):456-62.

[22] Azmi W, Sharma K, Sarma P, Mamat R, Anuar S, Sundar LS. Numerical validation of experimental heat transfer coefficient with SiO_2 nanofluid flowing in a tube with twisted tape inserts. Appl Therm Eng. 2014;73(1):296-306.

[23] Esfe MH, Saedodin S. Turbulent forced convection heat transfer and thermophysical properties of Mgo–water nanofluid with consideration of different nanoparticles diameter, an empirical study. J Therm Anal Calorim. 2015;119(2):1205-13.

[24] Ali HM. In tube convection heat transfer enhancement: SiO_2 aqua based nanofluids. J Mol Liq. 2020;308:113031.

[25] Abdolbaqi MK, Azwadi C, Mamat R. Heat transfer augmentation in the straight channel by using nanofluids. Case Studies in Thermal Engineering. 2014;3:59-67.

[26] Hemmat M, Saedodin S, Mahmoodi M, Experimental studies on the convective heat transfer performance and thermophysical properties of MgO–water nanofluid under turbulent flow. Exp Therm Fluid Sci. 2014;52:68-78.

[27] Wongcharee K, Eiamsa-Ard S. Enhancement of heat transfer using CuO/water nanofluid and twisted tape with alternate axis. Int Commun Heat Mass. 2011;38(6):742-8.

[28] Buongiorno J. Convective transport in nanofluids. 2006.

[29] Liu ZH, Liao L. Forced convective flow and heat transfer characteristics of aqueous drag-reducing fluid with carbon nanotubes added. Int J Therm Sci. 2010;49(12):2331-8.

[30] Nasiri A. M. Shariaty-Niasar., A. M. Rashidi. and R. Khodafarin., Effect of CNT structures on thermal conductivity and stability of nanofluid. Int J Heat Mass Transfer. 2012;55(5-6):1529-35.

[31] White FM. Viscous fluid flow. Second Edition ed. New York: McGraw-Hill, Inc.; 2006.

[32] Das SK, Putra N, Thiesen P, Roetzel W. Temperature dependence of thermal conductivity enhancement for nanofluids. J Heat Transfer. 2003;125(4):567-74.

[33] Xuan Y, Roetzel W. Conceptions for heat transfer correlation of nanofluids. Int J Heat Mass Transfer. 2000;43(19):3701-7.

[34] Drew DA, Passman SL. Theory of multicomponent fluids: Springer Science & Business Media; 2006.

[35] Maxwell JC. A Treatise on Electricity and Magnetism. Oxford, UK: Clarendon Press; 1881.

[36] Moffat RJ. Describing the uncertainties in experimental results. Exp Therm Fluid Sci. 1988;1(1):3-17.
[37] Roy R. A Primer on Taguchi Method, Van Noshtrand Reinhold Int. Co Ltd, New York. 1990.
[38] Gnielinski V. New equations for heat and mass-transfer in turbulent pipe and channel flow. Int Chem Eng. 1976;16(2):359-68.
[39] Dittus F, Boelter L. Heat transfer in automobile radiators of the tubular type. Int Commun Heat Mass. 1985;12(1):3-22.
[40] Duangthongsuk W, Wongwises S. An experimental study on the heat transfer performance and pressure drop of TiO_2-water nanofluids flowing under a turbulent flow regime. Int J Heat Mass Transfer. 2010;53(1–3):334-44.
[41] Kim D, Kwon Y, Cho Y, Li C, Cheong S, Hwang Y, et al. Convective heat transfer characteristics of nanofluids under laminar and turbulent flow conditions. Curr Appl Phys. 2009;9(2, Supplement):e119-e23.
[42] Kok PJAH, Kazarian SG, Lawrence CJ, Briscoe BJ. Near-wall particle depletion in a flowing colloidal suspension. J Rheol. 2002;46(2):481-93.
[43] Chou CS, Wu CY, Yeh CH, Yang RY, Chen JH. The optimum conditions for solid-state-prepared (Y3−xCex) Al_5O_{12} phosphor using the Taguchi method. Adv Powder Technol. 2012;23(1):97-103.